Inorganic Chemistry

ARTICLE

pubs.acs.org/IC

Tetra-2,3-pyrazinoporphyrazines with Externally Appended Pyridine Rings. 10. A Water-Soluble Bimetallic (Zn^{II}/Pt^{II}) Porphyrazine Hexacation as Potential Plurimodal Agent for Cancer Therapy: Exploring the Behavior as Ligand of Telomeric DNA G-Quadruplex Structures

Ilse Manet,[*,†] Francesco Manoli,[†] Maria Pia Donzello,[*,‡] Claudio Ercolani,[‡] Daniela Vittori,[‡] Luciano Cellai,[§] Annalisa Masi,[§] and Sandra Monti[*,†]

[†]Istituto per la Sintesi Organica e la Fotoreattività, Consiglio Nazionale delle Ricerche, via Gobetti 101, 40129 Bologna, Italy

[‡]Dipartimento di Chimica, Università degli Studi di Roma "La Sapienza", P.le A. Moro 5, 00185 Roma, Italy

[§]Istituto di Cristallografia, Consiglio Nazionale delle Ricerche, Area della Ricerca di Roma 1, 00015 Monterotondo Scalo, Rome, Italy

Supporting Information

ABSTRACT: The behavior of a bimetallic *water-soluble* (Zn^{II}/Pt^{II}) porphyrazine hexacation as ligand of G-quadruplex (G4) structures adopted by a human telomeric DNA sequence has been examined with different spectroscopic techniques. In K^+ rich solution the hexacationic Zn^{II} porphyrazine ligand bearing a peripheral cis-platin-like functionality changes the G-quadruplex conformational equilibrium of the human telomeric sequence 5′-d[AGGG(TTAGGG)$_3$]-3′ and drives it exclusively toward a very stable parallel G4 form in the complex with 2:1 stoichiometry. An increase of the melting temperature of more than 20 °C is observed in this complex compared to the G4 alone. On the contrary ligand binding to G-quadruplex of the same telomeric sequence in Na^+ rich solution neither markedly influences the predominant basket conformation nor confers increased thermal stability to the G4 structure.

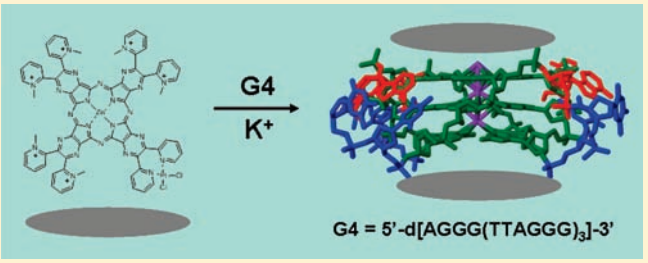

INTRODUCTION

The previous companion paper[1] reports on the synthesis, structure, and singlet oxygen photosensitizing properties of two novel classes of homo- and heterobimetallic derivatives of the free-base ligand tetrakis-2,3-[5,6-di-(2-pyridyl)pyrazino]porphyrazine, [LH_2], having general formulas [$(M'Cl_2)LM$] for the neutral species with M = Zn^{II}, $Mg^{II}(H_2O)$, Pd^{II}, and M′ = Pd^{II}, Pt^{II} (Scheme 1A) and [$(PtCl_2)(CH_3)_6LM]^{6+}$ for the hexacationic species neutralized by I^- ions with M = Zn^{II}, $Mg^{II}(H_2O)$, Pd^{II} (Scheme 1B). All the species have been characterized on the basis of their IR/UV−visible spectral features. ^1H and ^{13}C NMR spectral data indicate that the $PdCl_2$ and $PtCl_2$ exocyclic units in both the neutral and cationic species are peripherally coordinated to the nitrogens of two vicinal pyridine rings of a dipyridinopyrazine fragment in a manner similar to that previously observed with NMR in the pentapalladated analogues [$(PdCl_2)_4LM$] (M = Pd^{II}, Zn^{II}, $Mg^{II}(H_2O)$, Cu^{II}, Cd^{II}),[2,3] and, with single-crystal X-ray work, in the Pd^{II} and Pt^{II} derivatives of the precursor 2,3-dicyano-5,6-di(2-pyridyl)-1,4-pyrazine.[2,4]

All the species mentioned above behave in dimethylformamide as singlet oxygen photosensitizers of interest for photodynamic therapy (PDT), a well-known anticancer treatment.[5−10] Moreover, the series of externally platinated derivatives can also be seen as promising chemotherapeutic principles because of the cis-platin-like functionality. In this context a very relevant feature of the 6+ charged compounds is that they are water-soluble, a rare occurrence in the panorama of porphyrazine macrocycles. In this paper we explore the possibility of a third mode of action of the externally platinated 6+ charged compounds by examining their ability to act as ligands for DNA G-quadruplex structures in water.

G-quadruplex (G4) structures of guanine-rich DNA sequences consist of stacked planes of four guanosines, cyclically bound to each other via eight hydrogen bonds according to the Hoogsteen motif. Formation of the G4 structure is favored by the presence of monovalent cations like Na^+ and K^+.[11,12] Guanine-rich sequences are present in important regions of the human genome, like the telomeres at the end of the chromosomes and the promoter regions of several oncogenes.[11−16] The human telomere possesses a single stranded overhang at the 3′ end consisting prevalently of repeats of the GGGTTA sequence. Cellular senescence is related to telomere shortening during cell replication. An enzymatic

Received: March 12, 2011
Published: July 19, 2011

Scheme 1. Schematic Representation of the Neutral Bimetallic Species of Formula $[(M'Cl_2)LM]$ (M = Zn^{II}, $Mg^{II}(H_2O)$, Pd^{II}; M′ = Pd^{II}, Pt^{II}) (A) and the Related Platinated Hexacationic Species $[(PtCl_2)(CH_3)_6LM]^{6+}$ (M = Zn^{II}, $Mg^{II}(H_2O)$, Pd^{II}; neutralized by I^- ions) (B)

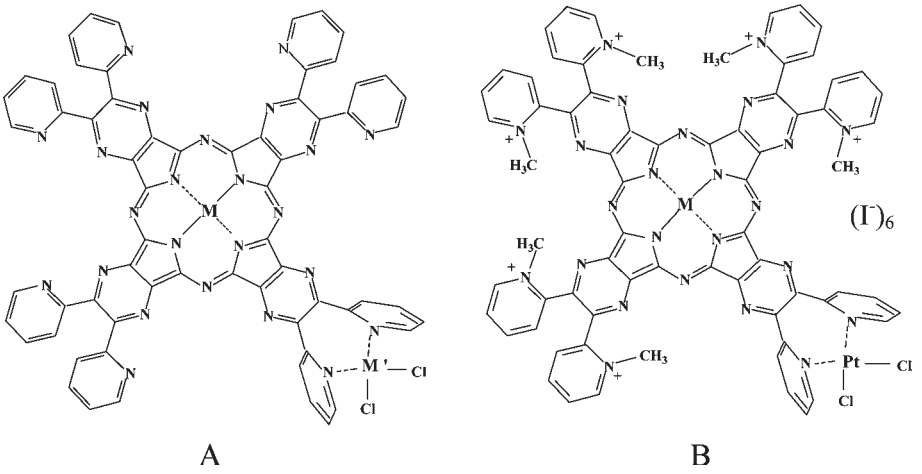

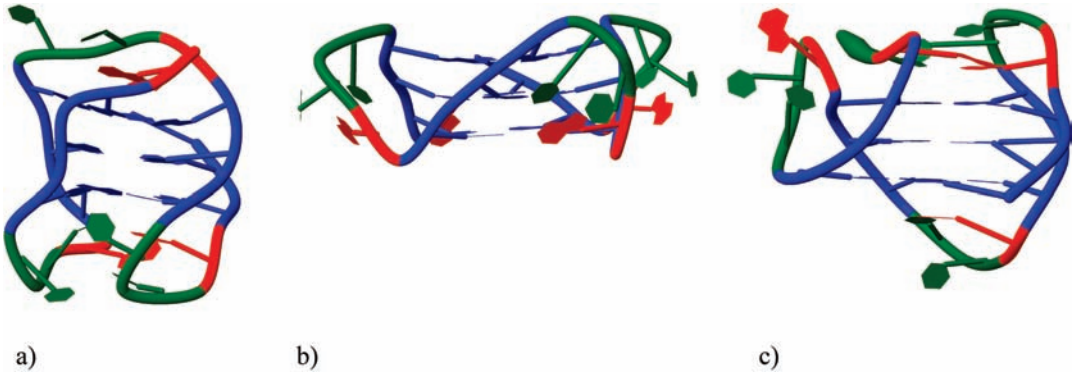

Figure 1. Cartoon representation of G4 conformations of (a) the 22-mer in Na^+ rich solutions (basket conformer, NDB 143D), (b) the 22-mer in the crystal structure in the presence of K^+ (parallel conformer, NDB 1KF1), and (c) a 23-mer in K^+ rich solutions ("(3 + 1) hybrid" conformer 1, NDB 2JSM). G, blue, T, green, A, red.

mechanism for telomere maintenance is mediated by a reverse transcriptase, called telomerase. Telomerase is overexpressed in about 85% of rapidly replicating cancer cells, thereby guaranteeing their "immortality".[17] It has been proven that the activity of this enzyme critically depends on the structural organization of these guanine-rich sequences.[17−21] In fact some ligands that bind to the G4 in solution stabilizing the structure also interfere with the biological processes involving guanine-rich sequences.[22,23] This fact has been observed not only for the telomeric sequences but also for other guanine-rich sequences present in the promoter regions of some oncogenes.[14,24] Consequently guanine-rich sequences have become a very promising target for the development of new anticancer drugs and attracted a lot of research interest during the past decade.[13−17,22,23]

We have recently published a short communication about the ability of the previously reported octacationic Zn^{II} complex $[(CH_3)_8LZn]^{8+}$ (hereafter shortly $[PzZn]^{8+}$) to form stable complexes with telomeric DNA in the G4 form.[25] This Zn^{II} cation has an aromatic planar tetrapyrazinoporphyrazine core with dimensions similar to those of the G4 tetrad and the presence of the positive charges was expected to favor binding due to the electrostatic interaction with the negatively charged DNA backbone.[26−28] We investigated the interaction of the octacation with the telomeric 22-mer sequence 5′-d[AGGG-$(TTAGGG)_3$]-3′ in K^+ rich solution. This sequence is known to adopt a conformation that strongly depends on the presence of ions: in Na^+ rich solutions a "basket" G4 structure is formed, with pairs of parallel and antiparallel GGG tracts linked by one diagonal and two lateral loops (Figure 1a);[29] in a K^+ containing crystal a propeller-type G4 folding is assumed, with four parallel GGG tracts and three TTA loops of the double-chain-reversal type (Figure 1b);[30] NMR showed that the same 22-mer in K^+ rich solutions adopts a "(3 + 1) hybrid" structure, as major conformer, featuring an arrangement of three parallel and one antiparallel GGG tracts, joined by one double-chain-reversal loop and two lateral loops (see Figure 1c for an example of hybrid conformation).[31,32] From our study some very interesting properties of the $[PzZn]^{8+}$−22-mer complexes emerged: the association of $[PzZn]^{8+}$ induces the almost exclusive formation of G4 with parallel structure, strongly stabilized compared to the free G4. These results were similar to those reported for a positively charged phthalocyanine derivative[33] and very different from those reported for binding of a tetramethylpyridiniumporphyrazine (both as free base and Zn^{II} complex), which in the

dx.doi.org/10.1021/ic200514z |Inorg. Chem. 2011, 50, 7403–7411

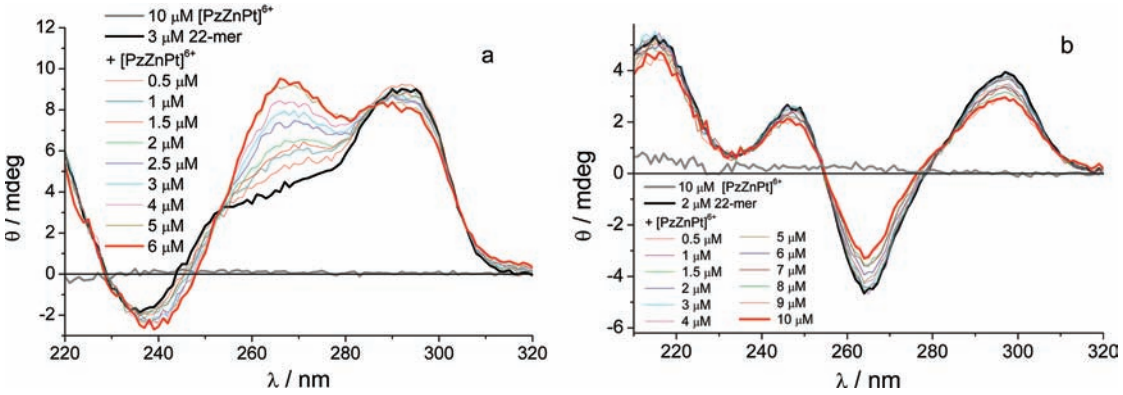

Figure 2. (a) Ellipticity (θ) of 3×10^{-6} M 22-mer solutions containing increasing concentrations of $[PzZnPt]^{6+}$ in TRIS/KCl buffer, pH 7.4; $[PzZnPt]^{6+} = (0.5, 1, 1.5, 2, 2.5, 3, 4, 5, 6) \times 10^{-6}$ M, (b) Ellipticity (θ) of 2×10^{-6} M 22-mer solutions containing increasing concentrations of $[PzZnPt]^{6+}$ in TRIS/NaCl buffer, pH 7.4; $[PzZnPt]^{6+} = (0.5, 1, 1.5, 2, 3, 4, 5, 6, 7, 8, 9, 10) \times 10^{-6}$ M; $d = 1.0$ cm, $T = 295$ K, the mixtures were kept in the dark at 22 °C for 3 days.

presence of K^+ preferentially induces formation of the antiparallel basket conformation in the complex.[27] All these compounds have a planar aromatic core of similar size. Nevertheless they differ for the position of the positive charges, residing on the core in the case of the tetramethylpyridiniumporphyrazine and residing on the peripheral substituents in the other cases.

In this article we focus on the binding of the bimetallic Zn^{II}/Pt^{II} hexacation (Scheme 1B, M = Zn^{II}; hereafter shortly $[PzZnPt]^{6+}$) to the same telomeric sequence, 5′-d[AGGG-(TTAGGG)$_3$]-3′ (22 mer). Among the platinated species the Zn^{II} hexacation shows good photosensitizing and fluorescence properties. Compared to $[PzZn]^{8+}$ the introduction of the exocyclic Pt^{II} unit confers lower symmetry and larger rigidity to the molecule and reduces the number of positive charges, possibly influencing affinity and/or binding modes for negatively charged G4 structures. Finally, it is worth noting that *cis*-Pt^{II} derivatives are known to interact prevalently at G-rich sites of duplex DNA forming intrastrand *cis*-$[PtX_2\{d(GpG)\}]$ adducts in cellular environment[34] further increasing the interest of understanding the interaction of $[PzZnPt]^{6+}$ with G-rich DNA sequences.

The interaction between the $[PzZnPt]^{6+}$ and the 22-mer was monitored by means of several spectroscopic techniques. Changes in the absorption, fluorescence, and circular dichroism (CD) clearly showed that association of the charged macrocycle to the 22-mer occurs. CD directly evidenced important conformational effects on the G4 structure upon binding of the Zn^{II}/Pt^{II} hexacation in K^+ rich solution. The observed effects are compared with those induced by the related octacation $[PzZn]^{8+}$ and with those obtained for binding of $[PzZnPt]^{6+}$ to G4 in Na^+ rich solutions.

EXPERIMENTAL SECTION

The hexacation $[PzZnPt]^{6+}$ in the form of the salt-like species $[PzZnPt](I_6)$ was prepared as reported in the previous companion paper.[1] The possible presence of impurities due to incomplete quaternization and/or multiple platination in the sample is not believed to be significant.[1] The telomeric sequence 5′-d[AGGG(TTAGGG)$_3$]-3′ (22-mer) was prepared by automated synthesis according to standard procedures.

Sample Preparation. The buffer for the spectroscopic measurements contained 10 mM TRIS and 100 mM KCl or NaCl. Excess of K^+ mimics physiological conditions of cellular compartments where K^+ is abundant. pH was corrected to a value of 7.4 with aliquots of HCl 3 N. For melting experiments only a 10 mM sodium cacodylate buffer with 100 mM KCl or NaCl was used. The pH of the buffer was corrected to a value of 7.4 with HCl 0.1 N. The 22-mer stock solution was heated at 90 °C for 15 min and then cooled to room temperature before use. The iodide salt of $[PzZnPt]^{6+}$ was dissolved up to a concentration of 1.2×10^{-5} M in these buffers. Aliquots of solution of the charged macrocycle and 22-mer solution in the same buffer were mixed together to prepare samples of varying molar ratio. Water was purified by passage through a Millipore Milli-Q system (Millipore SpA, Milan, Italy).

Photophysical Measurements. UV−visible absorption spectra were recorded on a Perkin-Elmer λ 950 spectrophotometer. Fluorescence spectra were obtained on a Spex Fluorolog 111A spectrofluorimeter. Right angle detection was used. CD spectra were obtained with a Jasco J-715 spectropolarimeter. Each CD spectrum was registered accumulating three scans with integration time of 1 s; scan rate was 100 nm/min for the 320−600 and 50 nm/min for the 220−350 nm range. In the 600−760 nm range six scans were accumulated with integration time of 2 s and the scan rate was 50 nm/min. All the measurements were carried out at 295 K in quartz cuvets of 2.0, 1.0, and 0.2 cm path length.

Titration experiments with detection of CD and absorption in the 320−800 nm range were performed at constant ligand and varying 22-mer concentrations. CD titrations below 320 nm were carried out keeping constant either the DNA or the ligand concentration. The best complexation model and the related association constants were determined by global analysis of multiwavelength data sets corresponding to 9−12 CD spectra of different mixtures in the 320−760 nm range, using the commercially available program SPECFIT/32 (version 3.0.40, TgK Scientific).[35] The multivariate optimization procedure is based on Singular Value Decomposition (SVD) and non linear regression modeling by the Levenberg−Marquardt algorithm. The deviations of the calculated ellipticity from the experimental values were minimized in a completely numerical procedure. See Supporting Information (SI) for further details.

In the melting experiments the temperature was changed in 1 °C steps and the ellipticity was read after 5 min. We applied a bandwidth of 2 nm and a response time of 8 s at 268 and 290 nm in K^+ rich solutions and at 295 and 260 nm in Na^+ rich solutions. The average of three readings was calculated. Error is estimated in ±0.05 mdeg.

RESULTS

Dimerization Equilibrium. It was previously shown that the octacationic species $[PzZn]^{8+}$ tends to aggregate in water solution.[36]

dx.doi.org/10.1021/ic200514z |*Inorg. Chem.* 2011, 50, 7403–7411

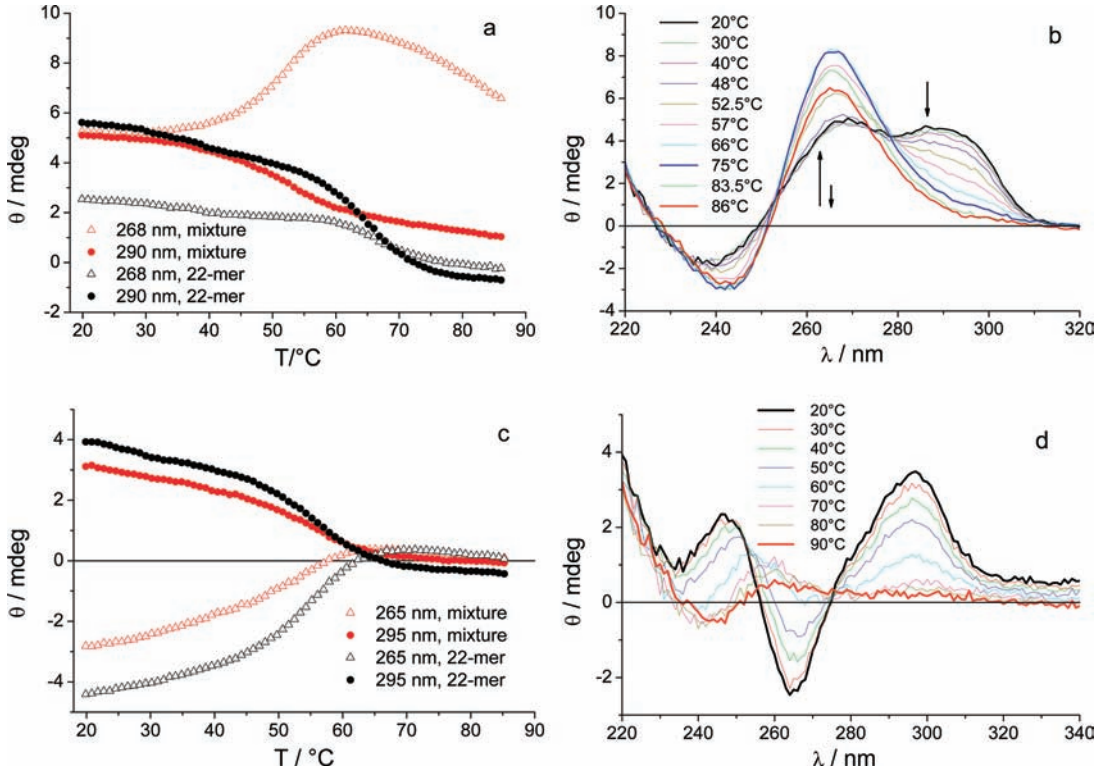

Figure 3. Ellipticity changes $\theta(T)$ of 22-mer 2.0×10^{-6} M solution (black) and of a mixture (red) of 22-mer 2.0×10^{-6} M and $[PzZnPt]^{6+}$ (1.0×10^{-5} M) in 10 mM Na cacodylate buffer of pH 7.4 (a) at 268 nm (Δ black, red) and 290 nm (● black, red) with 100 mM KCl and (c) at 265 nm (Δ black, red) and 295 nm (● black, red) with 100 mM NaCl. Temperature was changed 1 °C every 5 min; error on the readings was ±0.05 mdeg. CD spectra of the mixture of $[PzZnPt]^{6+}$ and 22-mer in presence of (b) 100 mM KCl and (d) 100 mM NaCl at different temperatures.

A dimerization constant of $\log(K_d/M^{-1}) = 6.6 \pm 0.5$ has been obtained.[25] The Q band of the absorption spectrum of the present hexacation $[PzZnPt]^{6+}$ in pure water has two maxima at 624 and 654 nm and the relative intensities of these peaks change upon dilution. These features are attributed also in this case to dimerization of the compound. We performed dilution experiments in water followed with absorption (Paragraph S1 in SI) to calculate the dimerization constant. Due to solubility problems this was not an easy task. Global analysis using SPECFIT/32 yielded an apparent dimerization constant $\log(K_d/M^{-1}) = 5.6 \pm 0.2$ (Durbin−Watson factor 1.5, relative error of fit 1.1%). The calculated spectra of the monomer and dimer show that the relative intensities of the peaks at 624 and 654 change upon monomerization. Further we observe for the dimer a strong hypochromic effect when compared to the isolated monomer.

Fluorescence. A 3×10^{-6} M solution of $[PzZnPt]^{6+}$ in 0.01 M TRIS buffer of pH 7.4 with 0.1 M KCl at 295 K exhibits a weak fluorescence band with maximum at 662 nm and a shoulder at 726 nm (see Figure S2 in SI). This emission is completely quenched upon addition of 22-mer. An electron transfer process, most likely from the guanosine residues, to the excited porphyrazine may be the reason for quenching as documented already in previous literature (see SI, paragraph S2).[37]

UV−visible Circular Dichroism. The 22-mer was titrated with $[PzZnPt]^{6+}$ in both K^+ and Na^+ rich solutions at 295 K monitoring CD in the 220−320 nm range, dominated by the G4 signal.[38] Figure 2a and b show the ellipticity changes observed in solutions stored in the dark at room temperature for 3 days in order to reach complete equilibration (see Figure S3 of SI for the CD spectra of the freshly prepared solutions). The pure 22-mer in K^+ rich buffer (Figure 2a, black curve) exhibits the typical spectral features of a mixture of 3 + 1 hybrid and basket conformers as main and minor species, respectively.[31,32,35] Addition of $[PzZnPt]^{6+}$ leads to an intensity increase of both the positive shoulder at 265 nm and the negative signal at 238 nm, the latter slightly shifting to the red, with a concomitant small decrease of the signal at 292 nm. The spectrum of the pure 22-mer (black curve, Figure 2b) in Na^+ rich buffer has the typical features of the basket conformer[31,35] and addition of $[PzZnPt]^{6+}$ only leads to small changes in the spectrum.

To understand the effect of the $[PzZnPt]^{6+}$ binding on the G4 stability we performed melting experiments monitoring the ellipticity at 290 and 268 nm for both the 22-mer alone (2.0×10^{-6} M) and the 22-mer in the presence of $[PzZnPt]^{6+}$ (1.0×10^{-5} M) in 10 mM Na cacodylate buffer of pH 7.4. The results are shown in Figure 3a and c for the K^+ rich and the Na^+ rich solutions, respectively.

We calculated $d\theta/dT$ from the data in Figure 3a and c to evidence the melting temperatures. The free 22-mer in K^+ rich solution melts at ca. 65 ± 2 °C, in agreement with data reported in literature.[39] The mixture $[PzZnPt]^{6+}$/22-mer presents instead two transition points. The first one at ca. 53 ± 2 °C, evidenced both at 268 and 290 nm, and a second one above 85 °C. We also registered the CD spectra of the mixture in the 220−320 nm region at various temperatures (see Figure 3b). It is evident from the spectral evolution that a complex with less stable G4 conformation, most likely the (3 + 1) hybrid one, undergoes a conformational transition assuming the parallel G4 structure, characterized by intense positive and negative peaks at 265 and 245 nm, respectively. Noticeably, the CD spectrum of the mixture at 75 °C features almost exclusively the G4 parallel

dx.doi.org/10.1021/ic200514z |Inorg. Chem. 2011, 50, 7403–7411

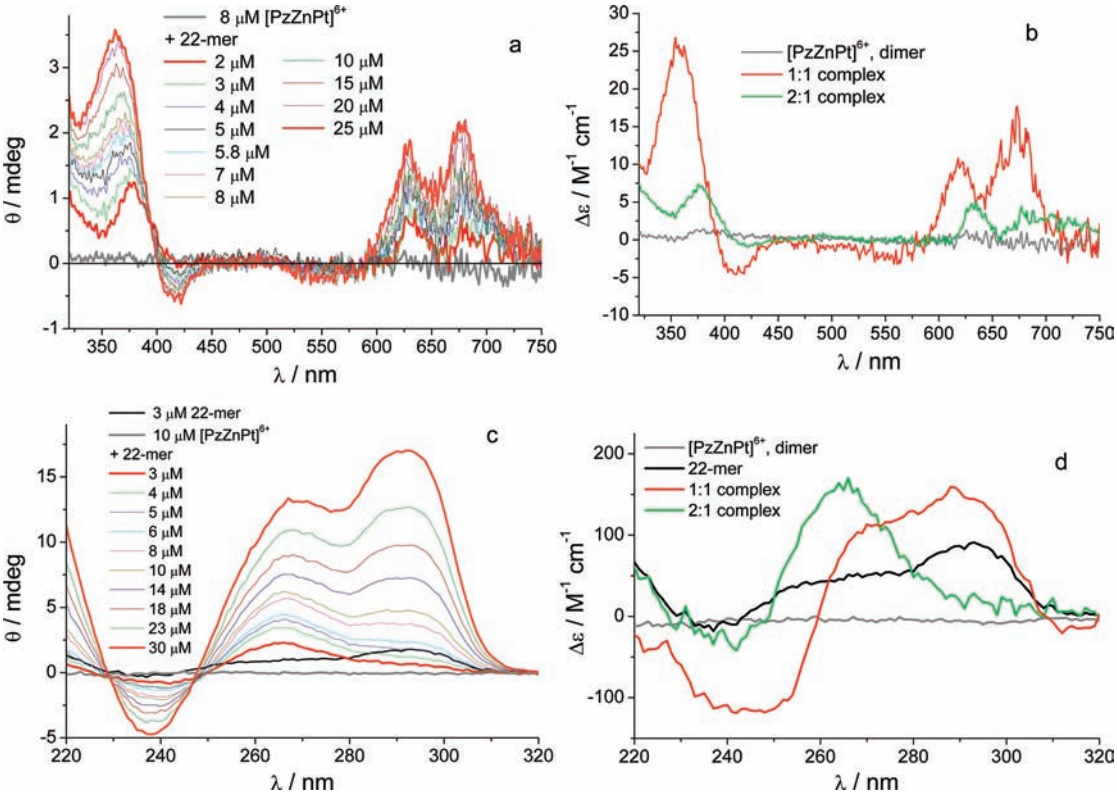

Figure 4. (a) Ellipticity (θ) of 8×10^{-6} M $[PzZnPt]^{6+}$ solutions with increasing 22-mer concentration $(0.2-2.5) \times 10^{-5}$ M in TRIS/KCl buffer of pH 7.4 at 295 K, $d = 2$ cm (average of 3 and 6 scans in the 320−600 nm and 600−750 nm ranges, respectively). (b) Calculated CD spectra ($\Delta\varepsilon$) of the free compounds and the complexes, $\log(K_{11}/M^{-1}) = 5.5 \pm 0.4$ and $\log(K_{21}/M^{-1}) = 12.3 \pm 0.4$. (c) Ellipticity ($\theta$) of 1×10^{-5} M $[PzZnPt]^{6+}$ solutions with increasing 22-mer concentration $(0.3-3) \times 10^{-5}$ M in TRIS/KCl buffer of pH 7.4 at 295 K, $d = 0.2$ cm. (d) Calculated CD spectrum ($\Delta\varepsilon$) of the complexes, $\log(K_{11}/M^{-1}) = 5.5$ and $\log(K_{21}/M^{-2}) = 11.9 \pm 0.2$. Note: the mixtures have been warmed at 60 °C for 10 min and cooled to 22 °C before measurement.

conformation.[14,40] Only for temperatures higher than 66 °C the parallel complex starts to disappear, but it is still surviving in large part at $T = 86$ °C. Upon cooling, the solution maintains the spectral features of the parallel conformation indicating that this G4 structure, once formed, is very stable (see SI, Figure S4). This behavior is not exhibited by the solution of 22-mer alone, which only shows decrease of the CD signal with increasing temperature (see SI, Figure S5). In the Na^+ rich buffer the melting monitored by CD at 265 and 295 nm evidenced a transition temperature around 55 °C for both 22-mer alone and the mixture. Looking at the spectral evolution of the latter with increasing temperature (Figure 3d) there is no conversion of the G4 basket conformation into the parallel form. We observed small ellipticity changes and above 50 °C the CD typical of the basket form abruptly disappears, the spectrum assuming the features of the single stranded DNA, similar to those observed for the 22-mer alone (see SI, Figure S6).

To gain further insights into the complexation process we titrated $[PzZnPt]^{6+}$ in K^+ rich buffer with the 22-mer, following the CD signal in the 320−600 nm range and the 600−750 nm range (Figure 4a).[41] $[PzZnPt]^{6+}$ is not chiral, thus the signal observed in this wavelength range is totally induced by the complexation to 22-mer. Global analysis of the multiwavelength data set in Figure 4a (see SI, paragraph S5) allowed determination of the stoichiometry, binding constants, and individual CD spectra of the most stable complexes. We included in the analysis the $[PzZnPt]^{6+}$ dimerization equilibrium with $\log(K_d/M^{-1}) = 5.6$ (for more information see SI, paragraph S1 and S5). Best fitting to the experimental data with satisfactory Durbin−Watson factors (DW) was obtained with a model involving two complexes of 1:1 and 2:1 $[PzZnPt]^{6+}$/22-mer stoichiometry in equilibrium with the free components.[42] The minimization procedure did not attain convergence with other binding models. The optimized binding constants resulted $\log(K_{11}/M^{-1}) = 5.5 \pm 0.4$ and $\log(K_{21}/M^{-1}) = 12.3 \pm 0.4$ (DW 2.3). The calculated CD of the individual complexes is shown in Figure 4b. We also monitored the CD in the UV region (see Figure 4c). It was necessary to fix the binding constant of the 1:1 complex in order to make the minimization procedure converge. Also the spectrum of the free 22-mer was fixed. The optimized binding constant resulted $\log(K_{21}/M^{-1}) = 11.9 \pm 0.2$ (DW 2.0) with $\log(K_{11}/M^{-1}) = 5.5$, in good agreement with the values obtained from data in the 320−750 nm region. The related CD of the individual complexes is shown in Figure 4d. The spectrum of the 2:1 species (with the positive band at 265 nm and the negative one at 245 nm) indicates the parallel G4 conformation is the dominating species, in agreement with the results of the melting experiments in Figure 3b, and the $\Delta\varepsilon$ values are coherent with data reported in literature.[40] The spectrum of the 1:1 complex evidences the presence of other additional conformations.

A series of similar experiments was performed in Na^+ rich buffer where the 22-mer adopts exclusively the basket structure, thereby allowing us to examine the interaction with the sole basket conformer.[29] So, we titrated $[PzZnPt]^{6+}$ with the 22-mer following the CD signal in the 320−750 nm range (Figure 5a)

dx.doi.org/10.1021/ic200514z |Inorg. Chem. 2011, 50, 7403–7411

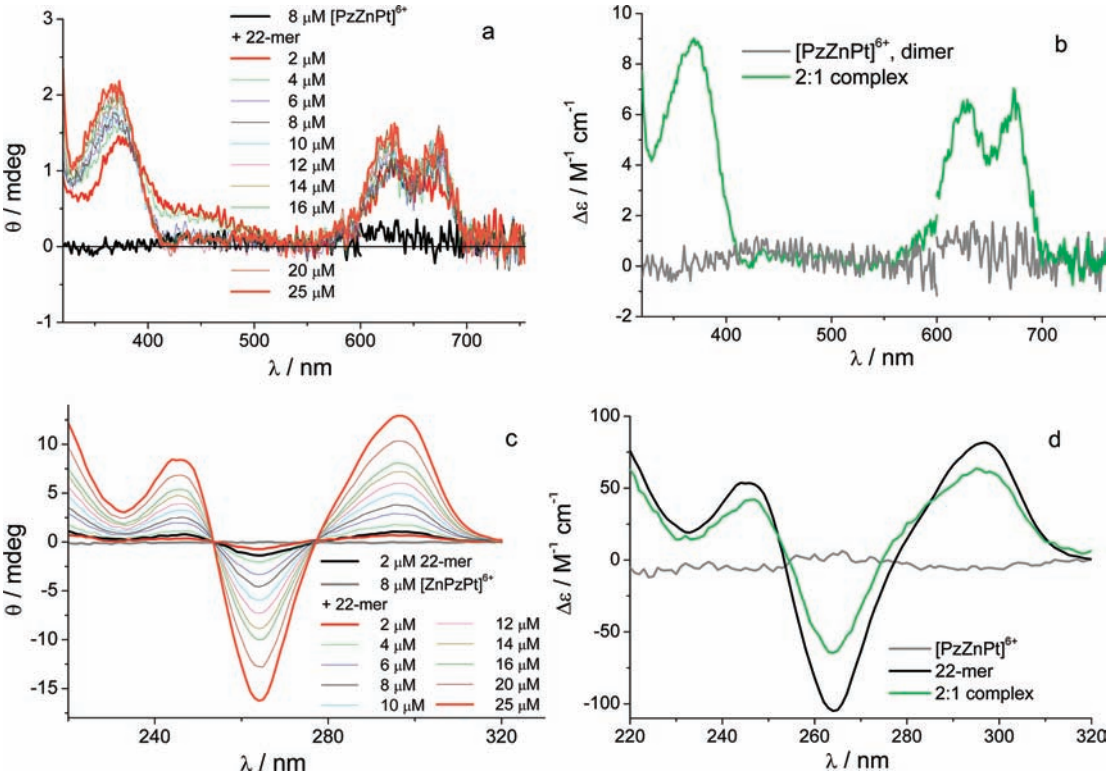

Figure 5. Ellipticity (θ) of 8×10^{-6} M $[PzZnPt]^{6+}$ solutions with increasing 22-mer concentration $(0.2-2.5) \times 10^{-5}$ M in TRIS/NaCl buffer of pH 7.4 at 295 K, (a) $d = 2$ cm (average of 3 and 6 scans in the 320−600 nm and 600−750 nm ranges, respectively), (c) $d = 0.2$ cm. (b) Calculated CD spectra ($\Delta\varepsilon$) of the free compound and the 2:1 complex, with $\log(K_{21}/M^{-2}) = 11.6 \pm 0.1$; the spectra corresponding to the two lowest 22-mer concentrations were not included in the analysis (see text). (d) Calculated CD spectra ($\Delta\varepsilon$) of the free compounds and the 2:1 complex, with $\log(K_{21}/M^{-2}) = 12.2 \pm 0.5$. Note: the mixtures have been warmed at 60 °C for 10 min and cooled to 22 °C before measurement.

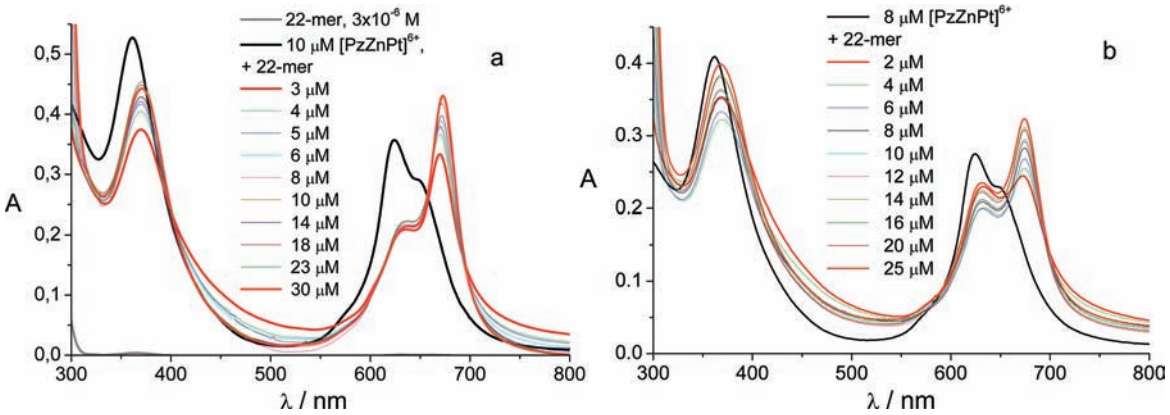

Figure 6. (a) Absorption spectra of a 1.0×10^{-5} M $[PzZnPt]^{6+}$ solutions with increasing 22-mer concentration (range $0.3-3) \times 10^{-5}$ M in TRIS/KCl buffer, pH 7.4, $d = 1.0$ cm. (b) Absorption spectra of a 8.0×10^{-6} M $[PzZnPt]^{6+}$ solutions with increasing 22-mer concentration (range $0.2-2.5) \times 10^{-5}$ M in TRIS/NaCl buffer, pH 7.4, $d = 1.0$ cm. Note: absorption spectra of $[PzZnPt]^{6+}$ alone are black.

and in the UV region (Figure 5c).[40] The data best-fitting procedure only converged assuming a binding model with the exclusive presence of the 2:1 complex and for the UV region yielded $\log(K_{21}/M^{-1}) = 12.2 \pm 0.5$ (DW 2.5). The CD shape (Figure 5d) confirmed that the G4 basket conformation is not appreciably perturbed by ligand association (see also Figure 2b). The 2:1 binding stoichiometry was confirmed by analysis of the data in the 320−750 nm region affording $\log(K_{21}/M^{-1}) = 11.6 \pm 0.1$ (DW factor 1.4). The spectra corresponding to the two lowest 22-mer concentrations were not included in this analysis because they are likely affected by the presence of higher order aggregates (see Discussion).

UV−visible Absorption. The absorption spectra of $[PzZnPt]^{6+}$/22-mer mixtures in buffered solution were taken in the 320−800 nm interval, where the $[PzZnPt]^{6+}$ signal is exclusively observed (Figure 6). As already found for the $[PzZn]^{8+}$ ligand,[25] quantitative analysis of absorption titration data was not successful either for the K^+ rich or the Na^+ rich solutions. We do not exclude the possibility of

dx.doi.org/10.1021/ic200514z |Inorg. Chem. 2011, 50, 7403–7411

aggregation phenomena, manifested in the high background above 700 nm with ligand over 22-mer excess; however specific spectral modifications observed along with the titration with 22-mer confirmed that complexation occurs. In K^+ rich medium the Soret band undergoes a red shift of 10 nm as well as a strong hypochromic change. The peak at 625 nm markedly decreases. Concomitantly the Q-band system shifts to the red showing maximum at 672 nm with a lower peak at 635 nm. The final orange spectrum in Figure 6a corresponds to a solution where ca. 94% of $[PzZnPt]^{6+}$ is bound either in 1:1 or in 2:1 stoichiometry ($[1:1] = 1.91 \times 10^{-6}$ M and $[2:1] = 3.73 \times 10^{-6}$ M calculated with the binding constants determined from 320 to 750 nm CD data, see also Figure S7 in SI). The initial red spectrum corresponds to 68% $[PzZnPt]^{6+}$ bound mainly in 2:1 complexes. It is deduced that the complexed hexacation in both stoichiometries is endowed with a similar Q-band system shifted to the red. This is also confirmed by the visible CD spectra of the complexes exhibiting a structured Q band with two maxima close to those of the absorption (see Figure 4b). In Na^+ rich solution the absorption changes induced by the addition of 22-mer are qualitatively similar: (a) the Soret peak undergoes a red shift of 8 nm as well as a hypochromic effect; (b) the peak at 625 nm decreases and, concomitantly, the Q band shifts to the red showing maxima at 631 and 674 nm. The orange spectrum corresponds to a solution where ca. 86% of $[PzZnPt]^{6+}$ is bound ($[2:1] = 3.46 \times 10^{-6}$ M, see Figure S12 in SI).

DISCUSSION

As outlined in the introduction, the compound $[PzZnPt]^{6+}$ presents as a potential plurimodal therapeutic agent in view of its photosensitizing properties, its cis-Pt functionality, and its G4-DNA binding ability. We will discuss the complexation to the G4 structures as deduced from the results of CD and absorption titration experiments, commenting on one hand the effect of the added cation and on the other hand the role of the structural differences between the hexacationic species and the octacationic one, $[PzZn]^{8+}$, of higher symmetry lacking the exocyclic Pt^{II} functionality. In analogy with $[PzZn]^{8+}$, also the $[PzZnPt]^{6+}$ ligand undergoes dimerization in aqueous solution. We have analyzed the titration data taking into account the ligand dimerization equilibrium.[43] The spectroscopic data indicate that binding of $[PzZnPt]^{6+}$ to the 22-mer occurs in both Na^+ and K^+ rich buffers. However the effects of complexation are very different in the two media. In the presence of K^+ association of $[PzZnPt]^{6+}$ strongly influences the G4 conformational equilibrium. In the 2:1 complex we observe the presence of the parallel conformer as dominating G4 species. This is not the case in the Na^+ containing buffer where the starting G4 conformation, i.e., the antiparallel basket form, is maintained in the complex even after heating. Moreover the parallel complex exhibits a much higher thermal stability than the 22-mer alone in K^+ rich medium, with melting temperature above 85 °C, whereas the antiparallel basket-like complex maintains the same melting temperature as the 22-mer alone in Na^+ rich medium (ca. 55 °C). Thus the effect of the $[PzZnPt]^{6+}$ ligand in both media is not the stabilization of the initial conformation. The induction of parallel G4 form by ligand binding seems to require the presence of K^+ as a cofactor and/or the presence of the hybrid G4 conformer as a prerequisite for promoting initial association and subsequent relaxation to the final geometry. A parallel conformation in K^+ rich solutions has been observed for other G-rich sequences with short loops[14,40] and for sequences with longer loops, such as the telomeric DNA, in the presence of ligands or in molecular crowding conditions.[33,44,45]

A diversified ligand-induced conformational effect on G4 is not the only difference between the two media. In K^+ rich solutions we have both 1:1 and 2:1 complexes in equilibrium, whereas in Na^+ rich buffer we have exclusively one complex of 2:1 stoichiometry keeping [ligand]/[22-mer] ratio below 4. In the first case we are likely observing binding to top and bottom tetrads of the parallel complex via stacking, whereas in the latter case we likely have binding at the basket grooves since the loops at top and bottom reasonably provide steric hindrance to ligand access to the tetrad. These results are different from those reported for one of the best known cationic porphyrin-based G4 ligands, TmPyP4.[46] In K^+ rich solution the latter ligand causes conformational changes in hybrid G4 structures of telomeric DNA favoring antiparallel structures and complexes of 4:1 ligand/DNA stoichiometry are formed.[47,48] Differently the crystal structure of a complex of TmPyP4 revealed the parallel G4 structure with TmPyP4 interacting with a lateral propeller loop and a T•A base bair on top of the 5′ external tetrad. No stacking was observed between tetrad and porphyrin aromatic ring.[49]

The results obtained for $[PzZnPt]^{6+}$ in K^+ rich solution show both similarities and differences from those reported for $[PzZn]^{8+}$. Concerning the 2:1 stoichiometry, the two ligands form complexes with similar spectroscopic properties in both the UV and the visible regions. Most likely they both interact by stacking of the central planar pyrazinoporphyrazine moiety with the terminal G-tetrads and this interaction is optimized in the parallel conformation. Actually in such geometry the three propeller loops do not confer substantial steric hindrance to ligand accommodation. Moreover the presence of the positive charges in the peripheral substituents allows optimization of the electrostatic interactions with the G4 phosphate groups present at the periphery of the top and bottom tetrad.[30] This factor represents an extra driving force for formation of the parallel G4 complex. At room temperature the complexation equilibrium is established slowly. Upon warming the solution the equilibration process accelerates leading eventually to almost exclusively parallel conformers, characterized by a high stability as testified by a melting temperature above 85 °C and persistence after cooling. Concerning the 1:1 complexes we observed markedly different CD spectra in the UV region with $[PzZnPt]^{6+}$ and $[PzZn]^{8+}$. It is possible that the structural difference in the two ligands causes diversified complexation geometries. Only six positive charges are present in the platinated compound and the Pt-bridged moiety is reasonably expected to possess some more rigidity if compared to the two pyridinium rings in the octacationic species. So lower electrostatic interaction as well as lower flexibility in the ligand structure may lead to different conformations for the 1:1 species. We do not exclude that the cis-platin function, known to interact with the grooves of B-DNA, may be involved in a different type of G4 binding. These features could also explain the observed difference in the binding constants of the Pt derivative, 1 order of magnitude lower than those of the octacationic species.

The weakness of the CD of the 2:1 complex in the visible region in the presence of K^+ compared to that of the 1:1 complex (Figure 4b), already observed for the octacationic ligand, may be due to a cancellation effect in a configuration where the two porphyrazine ligands stack as monomers on different diastereotopic faces of the top and bottom tetrads, thereby reasonably having a CD of opposite sign.[50,51]

With a porphyrazine excess of more than two we observe strong hypochromicity and band broadening in the absorption spectra, consistent with presence of higher order G4 complexes. It is possible that binding of cationic porphyrazines to grooves mediated by electrostatic interactions with the negatively charged phosphate groups promotes such phenomena with the porphyrazines acting as bridging ligands between parallel G4 units.[52] This type of interaction has also been evidenced in the crystal structure of TMPyP4 with parallel G4, where one molecule stacks with the tetrad and the second interacts with the groove.[49] The aggregation phenomenon is reasonably more important in Na^+ rich solutions because in this case grooves are favored binding sites instead of top and bottom tetrads.

CONCLUSION

Using CD and absorption spectroscopy we obtained a picture of the binding of the porphyrazine cation $[PzZnPt]^{6+}$ to an unmodified human telomeric sequence assuming G4 structure in K^+ rich solution. We compared the behavior of the hexacationic platinated species with that of the octacationic analog, lacking the exocyclic Pt^{II} functionality. Both molecules tend to aggregate in water and we took into account this feature when analyzing G4 complexation equilibria. Our study allowed us to assess that the cis-Pt^{II} functionality influences the G4 binding modalities, but does not compromise the potential of the hexacation as a promising therapeutic agent targeting G4. Accurate analysis of the circular dichroism in the UV as well as in the visible regions yielded information on the complex stoichiometry and the binding constants. The CD spectra of the complexes in 1:1 and 2:1 stoichiometry provided structural information on the G4 conformation in the bound state. Exclusive formation of the parallel G-quadruplex in K^+ rich solution was observed for the 2:1 complex. Both ligands exhibit good affinity for the parallel G-quadruplex form. The thermal stability of the parallel complexes is remarkable. The hexacationic species has a completely different complexation behavior toward G4 in the basket conformation in Na^+ rich solution, where neither ligand-induced formation of the parallel complex nor stabilization of the basket G4 structure were observed.

In conclusion, in the companion paper[1] we reported that $[PzZnPt]^{6+}$ is a good singlet oxygen photosensitizer while in the present paper we illustrated that it has promising features as G4 ligand and stabilizer in physiological-like (K^+ rich) conditions. In view of the cis-platin functionality we are currently studying the binding of $[PzZnPt]^{6+}$ and its octacationic analogue to duplex DNA. Further, in the frame of assessing the plurimodal potential of this molecule as drug we are currently investigating its photochemical behavior in the presence of biomolecules, its biological activity in vitro, and possible strategies to overcome the aggregation tendency.

ASSOCIATED CONTENT

Supporting Information. Additional text and figures. This material is available free of charge via the Internet at http://pubs.acs.org.

AUTHOR INFORMATION

Corresponding Authors

*E-mail: manet@isof.cnr.it. (I.M.); mariapia.donzello@uniroma1.it (M.P.D.)

ACKNOWLEDGMENT

We gratefully acknowledge the European Commission through the COST Action MP0802 that offers a stimulating environment for highly qualified discussions on the topic. M.P.D. also acknowledges scientific support by the Consorzio Interuniversitario di Ricerca in Chimica dei Metalli nei Sistemi Biologici (CIRCMSB) and financial help by the Ministero dell'Università e della Ricerca Scientifica (MIUR, PRIN 2007XWBRR4).

REFERENCES

(1) Donzello, M. P.; Vittori, D.; Viola, E.; Manet, I.; Mannina, L.; Cellai, L.; Monti, S.; Ercolani, C. *Inorg. Chem.* **2011**, *50*, DOI: 10.1021/ic200498s.

(2) Donzello, M. P.; Viola, E.; Cai, X.; Mannina, L.; Rizzoli, C.; Ricciardi, G.; Ercolani, C.; Kadish, K. M.; Rosa, A. *Inorg. Chem.* **2008**, *47* (9), 3903–3919.

(3) Donzello, M. P.; Viola, E.; Bergami, C.; Dini, D.; Ercolani, C.; Giustini, M.; Kadish, K. M.; Meneghetti, M.; Monacelli, F.; Rosa, A.; Ricciardi, G. *Inorg. Chem.* **2008**, *47* (19), 8757–8766.

(4) Cai, X. H.; Donzello, M. P.; Viola, E.; Rizzoli, C.; Ercolani, C.; Kadish, K. M. *Inorg. Chem.* **2009**, *48* (15), 7086–7098.

(5) Celli, J. P.; Spring, B. Q.; Rizvi, I.; Evans, C. L.; Samkoe, K. S.; Verma, S.; Pogue, B. W.; Hasan, T. *Chem. Rev.* **2010**, *110* (5), 2795–2838.

(6) O'Connor, A. E.; Gallagher, W. M.; Byrne, A. T. *Photochem. Photobiol.* **2009**, *85* (5), 1053–1074.

(7) Castano, A. P.; Mroz, P.; Hamblin, M. R. *Nat. Rev. Cancer* **2006**, *6* (7), 535–545.

(8) Szacilowski, K.; Macyk, W.; Drzewiecka-Matuszek, A.; Brindell, M.; Stochel, G. *Chem. Rev.* **2005**, *105* (6), 2647–2694.

(9) Macyk, W.; Franke, A. A.; Stochel, G. Y. *Coord. Chem. Rev.* **2005**, *249* (21−22), 2437–2457.

(10) DeRosa, M. C.; Crutchley, R. J. *Coord. Chem. Rev.* **2002**, *233*−*234*, 351–371.

(11) Patel, D. J.; Phan, A. T.; Kuryavyi, V. *Nucleic Acids Res.* **2007**, *35* (22), 7429–7455.

(12) Burge, S.; Parkinson, G. N.; Hazel, P.; Todd, A. K.; Neidle, S. *Nucleic Acids Res.* **2006**, *34* (19), 5402–5415.

(13) Balasubramanian, S.; Neidle, S. *Curr. Opin. Chem. Biol.* **2009**, *13* (3), 345–353.

(14) Qin, Y.; Hurley, L. H. *Biochimie* **2008**, *90* (8), 1149–1171.

(15) Hurley, L. H. *Nat. Rev. Cancer* **2002**, *2* (3), 188–200.

(16) Hurley, L. H. *Biochem. Soc. Trans.* **2001**, *29*, 692–696.

(17) De Cian, A.; Lacroix, L.; Douarre, C.; Temime-Smaali, N.; Trentesaux, C.; Riou, J. F.; Mergny, J. L. *Biochimie* **2008**, *90* (1), 131–155.

(18) Harley, C. B. *Nat. Rev. Cancer* **2008**, *8* (3), 167–179.

(19) Shi, D. F.; Wheelhouse, R. T.; Sun, D. Y.; Hurley, L. H. *J. Med. Chem.* **2001**, *44* (26), 4509–4523.

(20) Wheelhouse, R. T.; Sun, D. K.; Han, H. Y.; Han, F. X. G.; Hurley, L. H. *J. Am. Chem. Soc.* **1998**, *120* (13), 3261–3262.

(21) Sun, D. Y.; Thompson, B.; Cathers, B. E.; Salazar, M.; Kerwin, S. M.; Trent, J. O.; Jenkins, T. C.; Neidle, S.; Hurley, L. H. *J. Med. Chem.* **1997**, *40* (14), 2113–2116.

(22) Neidle, S. *Curr. Opin. Struct. Biol.* **2009**, *19* (3), 239–250.

(23) Ou, T. M.; Lu, Y. J.; Tan, J. H.; Huang, Z. S.; Wong, K. Y.; Gu, L. Q. *ChemMedChem* **2008**, *3* (5), 690–713.

(24) Brooks, T. A.; Hurley, L. H. *Nat. Rev. Cancer* **2009**, *9* (12), 849–861.

(25) Manet, I.; Manoli, F.; Donzello, M. P.; Viola, E.; Andreano, G.; Masi, A.; Cellai, L.; Monti, S. *Org. Biomol. Chem.* **2011**, *9* (3), 684–688.

(26) Alzeer, J.; Vummidi, B. R.; Roth, P. J. C.; Luedtke, N. W. *Angew. Chem., Int. Ed.* **2009**, *48* (49), 9362–9365.

(27) Goncalves, D. P. N.; Rodriguez, R.; Balasubramanian, S.; Sanders, J. K. M. *Chem. Commun.* **2006**, *45*, 4685–4687.

(28) Anderson, M. E.; Barrett, A. G. M.; Hoffman, B. M. *J. Inorg. Biochem.* **2000**, *80* (3−4), 257–260.
(29) Wang, Y.; Patel, D. J. *Structure* **1993**, *1* (4), 263–282.
(30) Parkinson, G. N.; Lee, M. P. H.; Neidle, S. *Nature* **2002**, *417* (6891), 876–880.
(31) Li, J.; Correia, J. J.; Wang, L.; Trent, J. O.; Chaires, J. B. *Nucleic Acids Res.* **2005**, *33* (14), 4649–4659.
(32) Ambrus, A.; Chen, D.; Dai, J. X.; Bialis, T.; Jones, R. A.; Yang, D. Z. *Nucleic Acids Res.* **2006**, *34* (9), 2723–2735.
(33) Alzeer, J.; Luedtke, N. W. *Biochemistry* **2010**, *49* (20), 4339–4348.
(34) Jamieson, E. R.; Lippard, S. J. *Chem. Rev.* **1999**, *99* (9), 2467–2498.
(35) Gray, R. D.; Li, J.; Chaires, J. B. *J. Phys. Chem. B* **2009**, *113* (9), 2676–2683.
(36) Bergami, C.; Donzello, M. P.; Monacelli, F.; Ercolani, C.; Kadish, K. M. *Inorg. Chem.* **2005**, *44* (26), 9862–9873.
(37) Steenkeste, K.; Enescu, M.; Tfibel, F.; Perree-Fauvet, M.; Fontaine-Aupart, M. P. *J. Phys. Chem. B* **2004**, *108* (32), 12215–12221.
(38) The buffer solution of the 22-mer solution has been heated to 90 °C and then cooled slowly before preparation of the mixtures.
(39) Lane, A. N.; Chaires, J. B.; Gray, R. D.; Trent, J. O. *Nucleic Acids Res.* **2008**, *36* (17), 5482–5515.
(40) Bugaut, A.; Balasubramanian, S. *Biochemistry* **2008**, *47* (2), 689–697.
(41) We did not exceed an excess of 4 in ligand/22-mer molar ratio to avoid unspecific binding.
(42) The DW test is very useful to check for the presence of autocorrelation in the residuals. This method is recommended for systematic misfit errors that can arise in titration experiments. It examines the tendency of successive residual errors to be correlated. The Durbin−Watson statistics ranges from 0.0 to 4.0, with an optimal midpoint value of 2.0 for uncorrelated residuals (i.e., no systematic misfit). In contrast to the Chi-squared statistics, which requires the noise in the experimental data to be random and normally distributed, the DW factor is meaningful even when the noise level in the data set is low. Because the factorized data usually have a significantly lower noise level than the original data, DW factor is ideal for the present type of data.
(43) The dimerization constant (pK = 5.55) is lower than that of $[PzZn]^{8+}$ (pK = 6.6). Because its determination was made difficult by the scarce stability of the aqueous solutions of $[PzZnPt]^{6+}$ we checked the influence of the value of K_d on the results of the analyses. Increasing K_d up to 1 order of magnitude did not result in change of either the best binding model or the qualitative features of the absolute spectra. Only the constant for formation of the 2:1 complexes slightly varied, but the changes were within the statistical uncertainty.
(44) Rezler, E. M.; Seenisamy, J.; Bashyam, S.; Kim, M. Y.; White, E.; Wilson, W. D.; Hurley, L. H. *J. Am. Chem. Soc.* **2005**, *127* (26), 9439–9447.
(45) Xue, Y.; Kan, Z. Y.; Wang, Q.; Yao, Y.; Liu, J.; Hao, Y. H.; Tan, Z. *J. Am. Chem. Soc.* **2007**, *129* (36), 11185–11191.
(46) TmPyP4 is cationic meso-tetrakis-(*N*-methyl-4-pyridyl)-porphyrin.
(47) Wei, C. Y.; Jia, G. Q.; Yuan, J. L.; Feng, Z. C.; Li, C. *Biochemistry* **2006**, *45* (21), 6681–6691.
(48) Martino, L.; Pagano, B.; Fotticchia, I.; Neidle, S.; Giancola, C. *J. Phys. Chem. B* **2009**, *113* (44), 14779–14786.
(49) Parkinson, G. N.; Ghosh, R.; Neidle, S. *Biochemistry* **2007**, *46* (9), 2390–2397.
(50) Davis, J. T. *Angew. Chem., Int. Ed.* **2004**, *43* (6), 668–698.
(51) Smith, F. W.; Lau, F. W.; Feigon, J. *Proc. Natl. Acad. Sci.* **1994**, *91* (22), 10546–10550.
(52) Higher order aggregation strongly affects the light transmission properties of the solutions, distorting the absorption signal vs buffer, but perturbs much less the dichroic features that result from a differential measurement in which scattering is better compensated. According to this the CD signals could be successfully analyzed.